CENTRE FOR **STOCHASTIC GEOMETRY**
AND ADVANCED **BIOIMAGING**

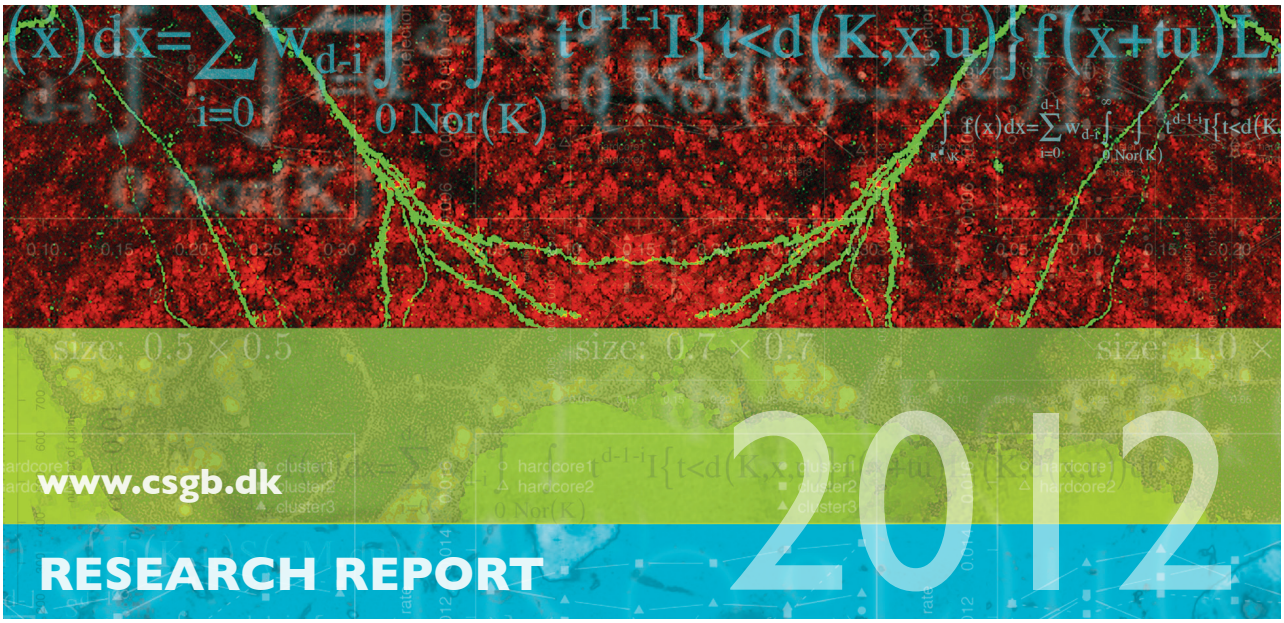

Jens Ledet Jensen, Merete Krog Raarup and Ege Rubak

Estimating protein-protein interaction affinity in single living cells using Förster resonance energy transfer measurements

No. 12, December 2012

Estimating protein-protein interaction affinity in single living cells using Förster resonance energy transfer measurements

Jens Ledet Jensen[1], Merete Krog Raarup[2] and Ege Rubak[3]

[1]Department of Mathematical Sciences, Aarhus University, Denmark, jlj@imf.au.dk
[2]Stereology and EM Laboratory, Aarhus University, Denmark, raarup@ki.au.dk
[3]Department of Mathematical Sciences, Aalborg University, Denmark, rubak@math.aau.dk

Abstract

Using Förster resonance energy transfer (FRET) images we study the possibility of estimating the equilibrium dissociation constant K_d and the intrinsic FRET efficiency E_m from single cells. We model the measurement uncertainty in the acquired images and use the method of total least squares for estimation based on the pixel values in the images. Considering a population of cells we demonstrate a variability in the estimates of K_d and E_m that cannot be explained by measurement noise and therefore points to systematic variation between images.

Keywords: Förster resonance energy transfer; protein-protein interaction; fluorescent proteins.

1 Introduction

In the literature several different Förster resonance energy transfer (FRET) measurements or indices have been proposed to indirectly study protein interactions at the nano scale (see e.g. Zal and Gascoigne (2004)). In Erickson et al. (2001) and Erickson et al. (2003) so called "three-cube" FRET was used to estimate the relative equilibrium dissociation constant K_d of two proteins, and later Chen et al. (2007) demonstrated a less challenging technique to estimate the relative K_d and the intrinsic FRET efficiency E_m in living cells using FRET. In that study a large number of cells were used. For each cell the pixel values were averaged and these averages were used for estimation. In this paper we study the abovementioned experiment in detail to understand the error terms and, in particular, to be able to estimate the interaction affinity and the intrinsic FRET efficiency from one cell only. This will open up for a much more dynamic study of living cells.

In the section *Theory* we describe the theoretical background of the experiment. The aim of the experiment was to estimate the equilibrium dissociation constant K_d

and the efficiency E_m. To study bias problems in different estimation procedures we need an understanding of the error terms in the acquired images. This is studied in the section *Error structure* and bias is studied in the section *Estimation bias*. In this paper we propose to use the total least squares method for estimation based on the pixel values for a single cell. The results from this estimation procedure are discussed in the section *Results*.

2 Theory

As we use the data from Chen et al. (2007) we refer to that paper for a detailed account of the materials used and how the data was acquired. Here we recall some notation and basic properties of FRET measurements. We are interested in studying the interaction between two proteins in living cells. To do this one protein is tagged with an acceptor fluorophore (fluorescent protein) and the other protein is tagged with a donor fluorophore. In the remainder the term *acceptor* denotes both the acceptor fluorophore and the protein tagged with the acceptor fluorophore. Similarly, *donor* refers to both the donor fluorophore and the protein tagged with the donor fluorophore. In the Chen et al. (2007) experiment the donor was FKBP12 tagged with Cerulean and the acceptor was Frb tagged with Venus and the cells used were HeLa cells.

A fluorophore can be excited by light of appropriate wavelengths (depending on the fluorophore type) and it then fluoresces by emitting light at longer wavelengths (again depending on the fluorophore type). If an acceptor is in close proximity (within $\sim 10\,\mathrm{nm}$) of an excited donor FRET may occur: the energy from the donor is transferred to the acceptor which then may deexcite by emission of light.

Using a microscope and lamp with appropriate filters three images were acquired: the acceptor image, $\mathrm{I_{AA}}$, where (mainly) the acceptor is excited and (mainly) the acceptor emission is measured; the donor image, $\mathrm{I_{DD}}$, where (mainly) the donor is excited and (mainly) the donor emission is measured; the FRET image, $\mathrm{I_{DA}}$, where (mainly) the donor is excited and (mainly) the acceptor emission is measured. Naturally, these images are measured with some noise and we let μ_{AA}, μ_{DD} and μ_{DA} denote the corresponding unknown noise-free images. The raw data provided to us by Chen et al. (2007) consists of a large collection of image triples where one or more cells are visible in each image. First, we have subtracted a background signal estimated from the darkest area of the image. Second, the cells have been extracted individually using a combination of thresholding and manual selection in the image software ImageJ (Rasband, 2012) such that the resulting images contain one cell each. Finally, for comparison with Chen et al. (2007) we only consider cells with an average value of $\mathrm{I_{AA}}$ below 5000 and the average value of $I_d/\mathrm{I_{AA}}$ between 0.2 and 5, where I_d is the total donor image as detailed below. Our final data set consists of a collection of image triples for 101 cells, see Figure 1 for an example.

Each of the three types of images may suffer from so-called cross talk (spectral bleed through). The cross talks for μ_{AA} and μ_{DD} are so small that they can be ignored. Thus μ_{AA} represents fluorescence from deexcitation of acceptors excited directly by the lamp only, and μ_{DD} represents fluorescence from deexcitation of donors excited directly by the lamp only. However, for μ_{DA} it is not appropriate to

ignore the cross talk. In this case the fluorescence originates from three different sources: emission from acceptors which have been excited by a nearby donor (the fluorescence of interest called the corrected FRET image μ_{F_c}), emission from donors which have been excited by the lamp (donor cross talk), emission from acceptors which have been excited directly by the lamp (acceptor cross talk). The corrected FRET image is

$$\mu_{F_c} = \mu_{\mathrm{DA}} - a\mu_{\mathrm{AA}} - d\mu_{\mathrm{DD}},$$

where a and d are the cross talk parameters. The corresponding measured image is $F_c = \mathrm{I}_{\mathrm{DA}} - a\mathrm{I}_{\mathrm{AA}} - d\mathrm{I}_{\mathrm{DD}}$. The cross talk parameters are estimated by considering cells only expressing either the acceptor or the donor as detailed in Section 3.2 and the supplementary material.

Besides the cross talk parameters two other parameters called G and k need to be estimated based on a control experiment. The details of estimating these are given in Chen et al. (2006) and we use the values obtained there: $G = 1.815$ and $k = 0.2168$.

If the two proteins enter in a bi-molecular interaction forming complexes (as is the case for FKBP12 and Frb in presence of the immunosuppressant rapamycin) the following equilibrium occurs

$$K_d[DA] = ([A] - [DA])([D] - [DA]) \tag{2.1}$$

where $[A]$ is the concentration of the acceptor, $[D]$ is the concentration of of the donor, $[DA]$ is the concentration of complexes with donor and acceptor and K_d is the equilibrium dissociation constant. We cannot measure these concentrations directly. Instead we consider μ_{AA} as a measure of the concentration $[A]$ such that the concentration is expressed in arbitrary fluorescent units AFU (the fluorescent units depend on the image setup). Then following Chen et al. (2007) we define the total donor image $\mu_d = (\mu_{DD} + \mu_{Fc}/G)/k$ with corresponding measured version $I_d = (I_{DD} + F_c/G)/k$ and the three concentrations in AFUs are:

$$[A] = \mu_{\mathrm{AA}}, \quad [D] = \mu_d, \quad [DA] = \frac{\mu_{Fc}}{E_m G k},$$

where E_m is the FRET efficiency and represents the fraction of excited donor-acceptor complexes for which energy is transferred to the acceptor. Solving the equilibrium equation (2.1) for the corrected FRET image μ_{F_c} as a function of the acceptor image μ_{AA} and the total donor image μ_d one obtains

$$\mu_E = \frac{E_m}{2\mu_d}\{\mu_{AA} + \mu_d + K_d - \sqrt{(\mu_{AA} + \mu_d + K_d)^2 - 4\mu_{AA}\mu_d}\}, \tag{2.2}$$

with the FRET efficiency image given by $\mu_E = \frac{\mu_{Fc}}{Gk\mu_d}$. The measured FRET efficiency image is $E = F_c/(GkI_d)$. The right hand side of (2.2) with measured images is denoted E_{pred}. Chen et al. (2007) find estimates of the equilibrium dissociation constant K_d and the FRET efficiency E_m by minimizing $(E - E_{\mathrm{pred}})^2$.

For the estimation method suggested in this paper we express the FRET image μ_{DA} as a function of the acceptor image μ_{AA} and the donor image μ_{DD}:

$$\mu_{DA} = \xi\{\mu_{AA} + \omega\mu_{DD} + \kappa - \sqrt{(\mu_{AA} + \omega\mu_{DD} + \kappa)^2 - 4\omega\mu_{AA}\mu_{DD}}\} + a\mu_{AA} + d\mu_{DD}, \tag{2.3}$$

where

$$\xi = \frac{E_m G k}{2}, \quad \omega = \frac{1}{k(1-E_m)}, \quad \kappa = \frac{K_d}{1-E_m}.$$

Combining this relation with a model for the measurement noise, estimates of the equilibrium dissociation constant K_d and the FRET efficiency E_m are obtained simultaneously with estimates of the acceptor and donor images μ_{AA} and μ_{DD}. First a square root transformation is used: $\mathrm{S_{AA}} = \sqrt{\mathrm{I_{AA}}}$, $\mathrm{S_{DD}} = \sqrt{\mathrm{I_{DD}}}$, $\mathrm{S_{DA}} = \sqrt{\mathrm{I_{DA}}}$ and $\gamma_{\mathrm{AA}} = \sqrt{\mu_{\mathrm{AA}}}$, $\gamma_{\mathrm{DD}} = \sqrt{\mu_{\mathrm{DD}}}$, $\gamma_{\mathrm{DA}} = \sqrt{\mu_{\mathrm{DA}}}$ and the estimates are found by minimizing a sum of terms of the form

$$\frac{1}{\sigma^2_{DA}}(\mathrm{S_{DA}} - \gamma_{\mathrm{DA}})^2 + \frac{1}{\sigma^2_{AA}}(\mathrm{S_{AA}} - \gamma_{\mathrm{AA}})^2 + \frac{1}{\sigma^2_{DD}}(\mathrm{S_{DD}} - \gamma_{\mathrm{DD}})^2.$$

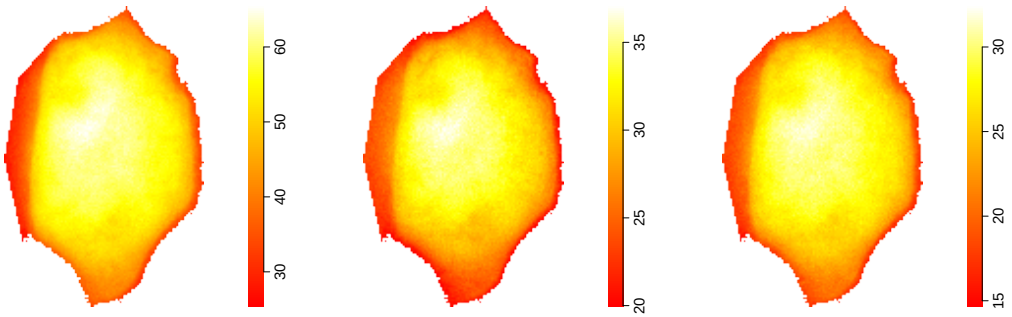

Figure 1: Data from one cell in the data set. From left to right showing the square root of: the acceptor image $\mathrm{S_{AA}} = \sqrt{\mathrm{I_{AA}}}$, the donor image $\mathrm{S_{DD}} = \sqrt{\mathrm{I_{DD}}}$ and the FRET image $\mathrm{S_{DA}} = \sqrt{\mathrm{I_{DA}}}$.

3 Results

3.1 Measurement noise

The three measured images $\mathrm{I_{AA}}$, $\mathrm{I_{DD}}$ and $\mathrm{I_{DA}}$ are noisy instances of the true contents μ_{AA}, μ_{DD} and μ_{DA}. Our aim is to estimate a nonlinear relationship among the true contents based on the measured images. Because of the non-linearity we need a fairly precise description of the error structure of the images. When measuring the light intensity during an exposure time t we assume the measurement to be proportional to the number of photons and expect the latter to be Poisson distributed. Let μ be the expected intensity per time unit. Then the mean and variance of the measurement become μt and $\sigma^2 \mu t$, where σ^2 is derived from the above proportionality. To be able to compare the images they are scaled by the inverse exposure time $1/t$ so that the mean and variance become μ and $\sigma^2 \mu / t$. This is our basic model for the measured images $\mathrm{I_{AA}}$, $\mathrm{I_{DD}}$ and $\mathrm{I_{DA}}$. Having the variance proportional to the mean can be handled in different ways. We choose here to perform a square root transformation giving the three images $S_{AA} = \sqrt{\mathrm{I_{AA}}}$, $S_{DD} = \sqrt{\mathrm{I_{DD}}}$ and $S_{DA} = \sqrt{\mathrm{I_{DA}}}$ with true contents $\gamma_{AA} = \sqrt{\mu_{AA}}$, $\gamma_{DD} = \sqrt{\mu_{DD}}$ and $\gamma_{DA} = \sqrt{\mu_{DA}}$. After the square root

transformation the mean and variance can be approximated by $\sqrt{\mu}$ and $\sigma^2/(4t)$. In the supplementary material we have illustrated the appropriateness of this model in two ways. For a cell expressing only the acceptor fluorophore, where we expect the relationship $\mu_{DA} = a\mu_{AA}$, or $\gamma_{DA} = a_0\gamma_{AA}$, Figure 6 shows the increase in variance of $\mathrm{I_{DA}}$ with $\mathrm{I_{AA}}$ and the stabilizing effect of the square root transformation. Figure 7 shows a close relation between the inverse exposure time $1/t$ and an independent estimate of the noise variance for the square root transformed images. The latter is obtained by looking at differences between neighbouring pixels based on an assumption of a slowly varying mean across a cell, see Figure 1 above. Based on the above observations all analyses of this paper are performed on square root transformed images and with a variance proportional to the inverse exposure time.

3.2 Systematic error

Based on the *acceptor only* cells and the *donor only* cells we discuss here the presence of systematic differences between the images.

For the *acceptor only* cells we have for the square root transformed images the relation $\gamma_{DA} = a_0\gamma_{AA}$. We have considered 88 cells and estimated a_0 in each of these. The average and empirical standard deviation of these 88 estimates are 0.188 and 0.0032. This standard deviation is much bigger than the standard deviation calculated from the measurement noise within a cell. The latter is on average 0.000037 for the 88 cells. Details of the calculations can be found in the supplementary material.

The situation is similar for the *donor only* cells. Here the relation is $\gamma_{DA} = d_0\gamma_{DD}$. For 66 cells the average and empirical standard deviation of the estimates of d_0 are 0.597 and 0.0030. The average of the standard deviation calculated from the measurement noise within a cell is 0.000096.

In the above investigations we thus see a variation among images with a relative magnitude (standard deviation divided by average) of the order 0.5 % to 2 %, which is much larger than what can be explained by measurement noise. The origin of these systematic variations from image to image is unknown.

3.3 Bias in K_d and E_m estimation using averages

Chen et al. (2007) estimated the equilibrium dissociation constant K_d and the FRET efficiency E_m using cell averages and the relation (2.2). However, the latter is a pixelwise relation, and since (2.2) is a nonlinear relation it does not in general hold with pixel values $(\mu_{AA}, \mu_{DD}, \mu_{DA})$ replaced by averages $(\bar{\mu}_{AA}, \bar{\mu}_{DD}, \bar{\mu}_{DA})$, where a bar signifies the average of the pixel values within a cell. Thus, using averages potentially introduces a bias in the estimation.

We can investigate the bias numerically by calculating a true image μ_{DA} through equation (2.3) from images μ_{AA} and μ_{DD} and given values of K_d and E_m. Next, we keep E_m fixed and find the value $\hat{K}_d^B$ that solves (2.3) with pixel values replaced by averages. We have done this with $K_d = 150$ and $E_m = 0.25$, and with possible instances of (μ_{AA}, μ_{DD}) given by $(\mathrm{I_{AA}}, \mathrm{I_{DD}})$ for 101 cells. The resulting values of $\hat{K}_d^B$ can be seen in Figure 2. The bias is mainly positive ($\hat{K}_d^B$ above 150) for ratios of $\bar{\mu}_{DD}/\bar{\mu}_{AA}$ below 0.7, and mainly negative for ratios above 0.7. The range of $\hat{K}_d^B$ is from 0 to 450, and overall, the bias is so large that it cannot be neglected.

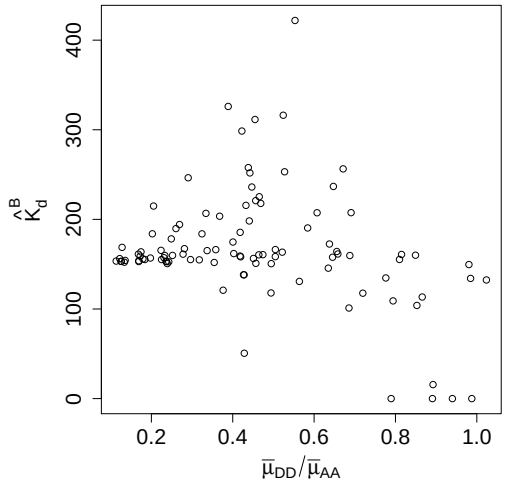

Figure 2: Bias from estimation based on cell averages. Estimates of K_d plotted against the ratio of averages $\bar{\mu}_{DD}/\bar{\mu}_{AA}$. The true value of K_d is 150.

3.4 Bias using ordinary least squares estimates of K_d and E_m

The estimation method of Chen et al. (2007), based on cell averages, is ordinary least squares (OLS) with the measured FRET efficiency E as the response and (I_{AA}, I_d) as the predictor variables. Using this method on pixel values instead of averages potentially leads to another bias problem due to measurement errors in the predictor variables. In this section we study this bias and compare with the method proposed in the present paper, namely the use of total least squares (TLS) where the true contents μ_{AA} and μ_{DD} are estimated for each pixel in the images.

We have simulated images including measurement noise with $E_m = 0.25$ and $K_d = 150$. For this we use actual cell values (I_{AA}, I_{DD}) as possible instances of (μ_{AA}, μ_{DD}) and calculate μ_{DA} from equation (2.3). Transforming to $(\gamma_{AA}, \gamma_{DD}, \gamma_{DA})$ we add noise similar to the noise level in the observed cells to obtain simulated observed images (S_{AA}, S_{DD}, S_{DA}), and then find the estimates $\hat{E}_m$ and $\hat{K}_d$ of E_m and K_d using either OLS or TLS. In Figure 3 left part we have simulated once for 101 different cells, and in the middle part we have simulated 100 times for each of the 101 cells and taken averages. In the right part of Figure 3 we show the 100 simulated values for one cell. It is clear from these figures that the OLS estimation method produces biased results, where the amount of bias depends on the actual cell. Contrary to this the TLS method has a negligible bias.

3.5 Total least squares estimation

The data shows a large systematic variation in the noise free images γ_{AA} and γ_{DD}. This is illustrated in Figure 1 where the variation across the cell is of the order 10 times larger than the pixel to pixel variation.

The systematic variation is what causes the bias using averages of pixel values for estimation as discussed in the section *Bias using averages*. On the other hand

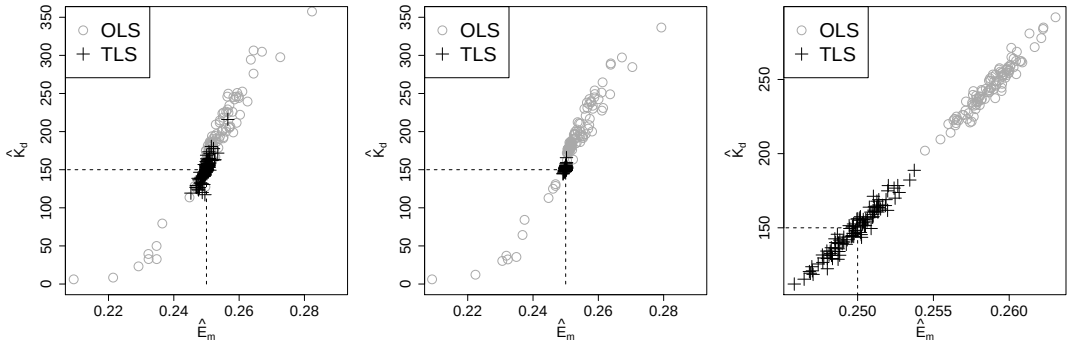

Figure 3: Comparison of OLS and TLS estimates of E_m and K_d for simulated data generated with $E_m = 0.25$ and $K_d = 150$ (marked by dashed lines in the figures). Left: Results for one simulated data set with 101 different cells. Middle: Average of 100 replications of simulated data for each of the 101 cells. Right: Estimates from 100 simulations based on the single cell shown in Figure 1.

this variation is exactly what is needed for being able to base the estimation on the pixel values for a single cell.

The total least squares estimates of K_d and E_m for all of the 101 cells have been found as explained in the section *Theory* and detailed in the supplementary material. Figure 4 shows the estimates. The left subfigure is a plot of the estimate $\hat{K}_d$ of the equilibrium dissociation constant against the estimate $\hat{E}_m$ of the FRET efficiency. The figure shows a positive correlation among the two estimates. This simply reflects the way that K_d and E_m enter the relationship (2.3). There is a surprisingly large variation in the estimates from one cell to another. The variation in the estimates due to measurement errors, as illustrated in Figure 3, is very small as compared to the variation seen in Figure 4. As described in subsection *Systematic error* there is some systematic variation from image to image and such an effect will surely give rise to some variation in the cell based estimates of (K_d, E_m).

We have also considered how well the model (that is, the error structure and the relation (2.3)) fits the data. We have looked at images of the residuals and found that for some cells there seems to be systematic deviations from the model predictions. Figure 5 shows an example with a cell with a good fit and another cell with a bad fit to the model. We have found that the quality of the fit correlates well with the raw sum of squared residuals (RSSD), that is, the sum over pixels of $(S_{DA} - \hat{\gamma}_{DA})^2$. The right subfigure in Figure 4 shows the estimates of K_d and E_m for those cells having a good fit defined by a value of RSSD below 0.10. As can be seen this removes some of the cells with $\hat{K}_d = 0$ but otherwise only slightly reduces the variation in the estimates.

The above findings show that all of the cells cannot be described by the same value of the parameters (K_d, E_m). Whether the variation from cell to cell is due to random effects causing systematic differences between images or whether the theory needs to be adjusted calls for further experiments. For the 60 selected cells shown in the right part of Figure 4 the estimates vary considerably. The average of the 60 values of $\hat{E}_m$ is 0.202 and the standard deviation is 0.05, and the average of $\hat{K}_d$ is 84.4 with a standard deviation of 133.1.

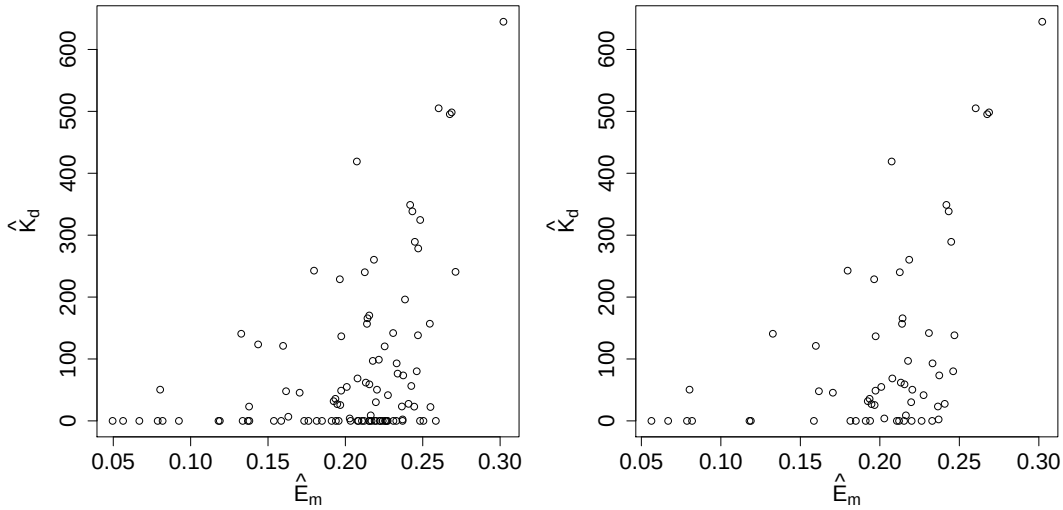

Figure 4: Values of $(\hat{E}_m, \hat{K}_d)$. Left: Estimates for all 101 cells. Right: Only cells with $RSSD < 0.1$

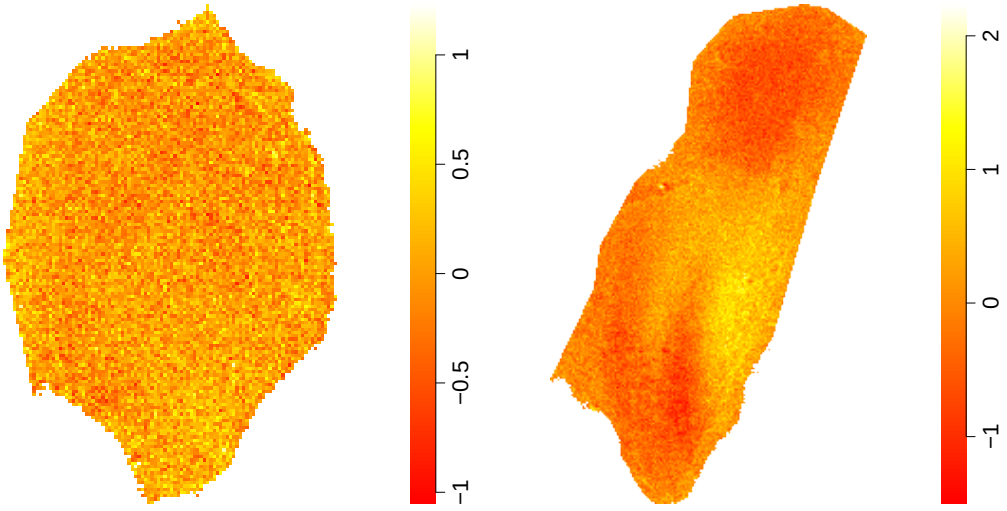

Figure 5: Residuals for two different cells. Left: Reasonable fit. Right: Poor fit showing clear systematic deviations form the model.

4 Summary and conclusion

We have found that the measurement noise in the images scales with the mean, or, alternatively, that the square root transformed images has constant variances. Furthermore, this variance is proportional to the inverse exposure time. Also, we have found that apart from the measurement noise there are systematic differences from image to image giving rise to variation in estimates much higher than the variation due to measurement noise. The origin of these differences is unclear, but must be related to the way the images are acquired or the way the fluorophores are excited.

We have found that using cell averages for the estimation of the equilibrium dissociation constant K_d and the FRET efficiency E_m leads to biased estimates. This bias is to some degree dependent on the donor to acceptor ratio. Also, we have seen that to produce unbiased estimates one needs to use the total least squares solution as opposed to the ordinary least squares method.

We have found that single cells can indeed be used for establishing the equilibrium dissociation constant K_d and the FRET efficiency E_m, that is, there is sufficient variation in the donor and acceptor images to provide information on these parameters. The variation in the estimates of K_d and E_m from cell to cell is quite large, which appears to be due to the aforementioned systematic differences between images.

Acknowledgments

We are grateful to Chen et al. (2007) for granting us access to their data. Supported by the Danish Natural Science Research Council, grant 09-072331, "Point process modelling and statistical inference", and by the Centre for Stochastic Geometry and Advanced Bioimaging, funded by a grant from the Villum Foundation.

Supplementary material

A Error structure

To learn about the error structure we have used cells expressing one fluorophore-tagged protein only. For these there is a simple relation among the images. We use the square root transformed images S_{AA}, S_{DD} and S_{DA}, and assuming a constant measurement variance we denote these by σ^2_{AA}, σ^2_{DD} and σ^2_{DA}.

In the *acceptor only* images the signal in the FRET image is due to crosstalk and we have the relation $\mu_{DA} = a\mu_{AA}$ or $\gamma_{DA} = a_0\gamma_{AA}$ with $a_0 = \sqrt{a}$. An asymptotic unbiased estimate of a_0 is obtained as $\hat{a}_0 = \sum_i S_{DAi} / \sum_i S_{AAi}$, where i in an index for pixels of the images. The estimate has asymptotically mean a_0 and standard deviation $\mathrm{sd}(\hat{a}_0) = \{(\sigma^2_{DA} + a\sigma^2_{AA})/(n\bar{S}^2_{AA})\}^{1/2}$, where n is the number of pixels. An estimate s_A of this standard deviation is obtained based on the empirical variance of $S_{DA} - \hat{a}_0 S_{AA}$. Table 1 contains means and standard deviations of $\hat{a}_0$, and s_A for 88 cells. The assumption of a constant variance after the square root transformation of

Table 1: Results for cells expressing acceptor or donor only.

$\hat{a}_0$	s_A	$\hat{d}_0$	s_D
0.655 (0.00791)	0.000312 (0.000082)	0.451 (0.0139)	0.000228 (0.000054)

the images is illustrated in Figure 6. The left part is a plot of the FRET image I_{DA} against acceptor image I_{AA} and shows an increase in the variance with increasing amount of acceptor. The middle figure shows in more detail this increase using a boxplot of $I_{DA} - \hat{a} I_{AA}$ based on a grouping of I_{AA}. The right part is a similar boxplot after the square root transformation, that is, a boxplot of $S_{DA} - \hat{a}_0 S_{AA}$ based on a grouping of S_{AA}.

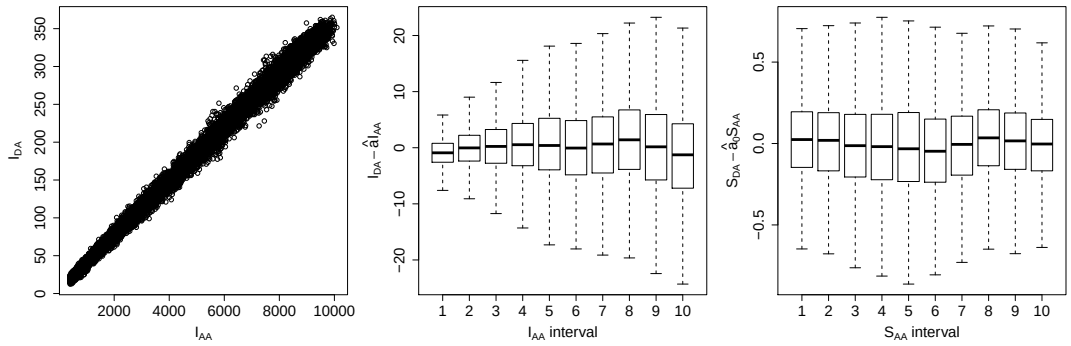

Figure 6: Data for a cell expressing the acceptor fluorophore only. Left: $\mathrm{I_{DA}}$ plotted against $\mathrm{I_{AA}}$. Middle: Boxplots of $\mathrm{I_{DA}} - \hat{a}\mathrm{I_{AA}}$ where the data is grouped by dividing the range of $\mathrm{I_{AA}}$ in 10 equally sized intervals. Right: Boxplots of $\mathrm{S_{DA}} - \hat{a}_0\mathrm{S_{AA}}$ where the data is grouped by dividing the range of $\mathrm{S_{AA}}$ in 10 equally sized intervals.

For the *donor only* images the signal in the FRET image is also due to crosstalk and we have the relation $\mu_{DA} = d\mu_{DD}$ or $\gamma_{DA} = d_0\gamma_{DD}$ with $d_0 = \sqrt{d}$. An asymptotic unbiased estimate of d_0 is obtained as $\hat{d}_0 = \sum_i S_{DAi} / \sum_i S_{DDi}$. The estimate has asymptotically mean d_0 and standard deviation $\{(\sigma^2_{DA} + d\sigma^2_{DD})/(n\bar{S}^2_{DD})\}^{1/2}$. An estimate s_D is obtained analogously to the acceptor only case. Table 1 contains means and standard deviations of $\hat{d}_0$, and s_D for 66 cells.

To study the size of the measurement errors in the square root transformed images S_{AA}, S_{DD} and S_{DA} we have estimated the variances σ^2_{AA}, σ^2_{DD} and σ^2_{DA} from differences of two neighbouring pixels. Figure 7 left shows a good agreement between the estimated variance and the inverse exposure time as expected from a Poisson variation (see subsection *Measurement noise*). For the total least squares estimation we do not need the absolute variances, but rather the ratios $\sigma^2_{DD}/\sigma^2_{AA}$ and $\sigma^2_{DA}/\sigma^2_{AA}$. The latter ratios are shown in the right part of Figure 7 and the prediction of these ratios from the inverse exposure times is very good.

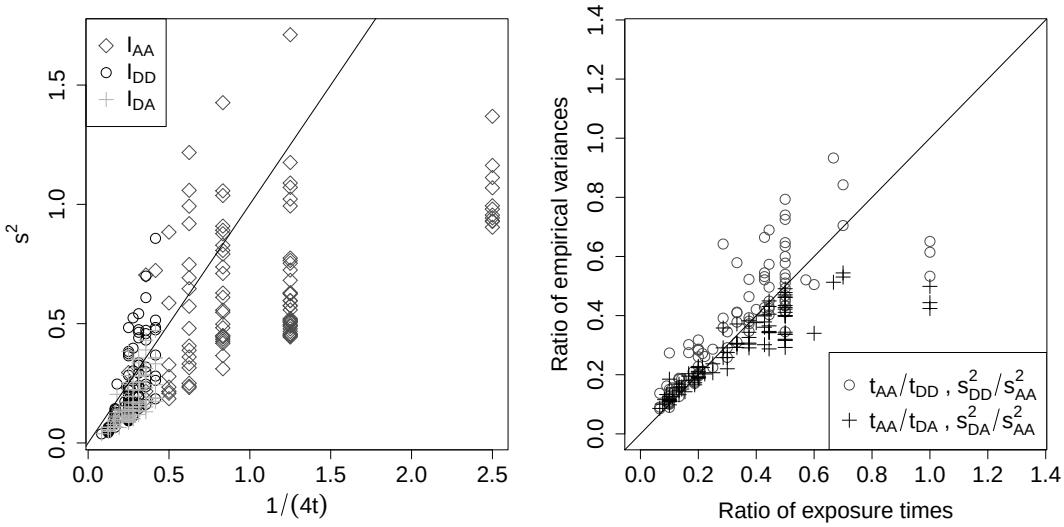

Figure 7: Comparison of inverse exposure times and the empirical noise variance (estimated from the pixel variation within an image). Left: Direct comparison of empirical noise variance (ordinate) and $1/(4t)$ expected under Poisson variation (abscissa). Right: Comparison of ratios of empirical variances and ratios of exposure times.

B Estimation algorithm

Recalling our notation the noise free images are μ_{AA} (acceptor), μ_{DD} (donor) and μ_{DA} (FRET). We have found that in each of the three measured images the variance of the noise scales with the mean value. An easy way to incorporate this into a model is to consider the square root of the images, denoted by S_{AA}, S_{DD} and S_{DA} with means $\gamma_{AA} = \sqrt{\mu_{AA}}$, $\gamma_{DD} = \sqrt{\mu_{DD}}$ and $\gamma_{DA} = \sqrt{\mu_{DA}}$. Our basic model for the noise is

$$S_{AA} \sim N(\gamma_{AA}, \sigma^2_{AA}), \quad S_{DD} \sim N(\gamma_{DD}, \sigma^2_{DD}), \quad S_{DA} \sim N(\gamma_{DA}, \sigma^2_{DA}), \tag{B.1}$$

The equilibrium equation (2.3) expressed with the square root transformed terms is

$$\gamma_{DA} = \sqrt{\xi\{T - \sqrt{T^2 - 4U}\} + a\gamma^2_{AA} + d\gamma^2_{DD}}, \tag{B.2}$$
$$T = \gamma^2_{AA} + \omega\gamma^2_{DD} + \kappa, \quad U = \omega\gamma^2_{AA}\gamma^2_{DD}$$

where

$$\xi = \frac{E_m G k}{2}, \quad \omega = \frac{1}{k(1 - E_m)}, \quad \kappa = \frac{K_d}{1 - E_m}.$$

Thinking of S_{DA} as the 'response' and S_{AA} and S_{DD} as 'explanatory', we cannot use ordinary least squares due to the noise in the images of the latter two. Instead we use total least squares where $(\gamma_{AA}, \gamma_{DD})$ are estimated for each pixel in the image (Markovsky and Huffel, 2007). The algorithm we use for solving this problem iterates between updating (Newton-Raphson step) the images γ_{AA} and γ_{DD} for a fixed value of (E_m, K_d), and updating (E_m, K_d) for fixed images γ_{AA} and γ_{DD}. Thus we minimize

$$Q = \sum \left\{ \frac{(S_{AA} - \gamma_{AA})^2}{\sigma^2_{AA}} + \frac{(S_{DD} - \gamma_{DD})^2}{\sigma^2_{DD}} + \frac{(S_{DA} - \gamma_{DA})^2}{\sigma^2_{DA}} \right\}, \tag{B.3}$$

where the sum is over all the pixels of the images. To update γ_{AA} and γ_{DD} we need the derivatives

$$\frac{\partial \gamma_{DA}}{\partial \gamma_{AA}} = \frac{\gamma_{AA}}{\gamma_{DA}} \frac{\partial \mu_{DA}}{\partial \mu_{AA}}, \qquad \frac{\partial \gamma_{DA}}{\partial \gamma_{DD}} = \frac{\gamma_{DD}}{\gamma_{DA}} \frac{\partial \mu_{DA}}{\partial \mu_{DD}},$$
$$\frac{\partial^2 \gamma_{DA}}{\partial \gamma_{AA} \partial \gamma_{AA}} = \frac{\mu_{DA} \frac{\partial \mu_{DA}}{\partial \mu_{AA}} + 2\mu_{DA}\mu_{AA} \frac{\partial^2 \mu_{DA}}{\partial \mu_{AA} \partial \mu_{AA}} - \mu_{AA} (\frac{\partial \mu_{DA}}{\partial \mu_{AA}})^2}{\gamma_{DA}\mu_{DA}},$$
$$\frac{\partial^2 \gamma_{DA}}{\partial \gamma_{DD} \partial \gamma_{DD}} = \frac{\mu_{DA} \frac{\partial \mu_{DA}}{\partial \mu_{DD}} + 2\mu_{DA}\mu_{DD} \frac{\partial^2 \mu_{DA}}{\partial \mu_{DD} \partial \mu_{DD}} - \mu_{DD} (\frac{\partial \mu_{DA}}{\partial \mu_{DD}})^2}{\gamma_{DA}\mu_{DA}},$$
$$\frac{\partial^2 \gamma_{DA}}{\partial \gamma_{AA} \partial \gamma_{DD}} = \frac{2\mu_{DA}\gamma_{AA}\gamma_{DD} \frac{\partial^2 \mu_{DA}}{\partial \mu_{AA} \partial \mu_{DD}} - \gamma_{AA}\gamma_{DD} \frac{\partial \mu_{DA}}{\partial \mu_{AA}} \frac{\partial \mu_{DA}}{\partial \mu_{DD}}}{\gamma_{DA}\mu_{DA}},$$

with

$$\frac{\partial \mu_{DA}}{\partial \mu_{AA}} = \xi[1 - \frac{\mu_{AA} - \omega\mu_{DD} + \kappa}{\sqrt{T^2 - 4U}}] + a,$$
$$\frac{\partial \mu_{DA}}{\partial \mu_{DD}} = \omega\xi[1 - \frac{\omega\mu_{DD} - \mu_{AA} + \kappa}{\sqrt{T^2 - 4U}}] + d,$$
$$\frac{\partial^2 \mu_{DA}}{\partial \mu_{AA} \partial \mu_{AA}} = -4\xi \frac{\kappa\omega\mu_{DD}}{\sqrt{T^2 - 4U}^3},$$
$$\frac{\partial^2 \mu_{DA}}{\partial \mu_{DD} \partial \mu_{DD}} = -4\omega^2\xi \frac{\kappa\mu_{AA}}{\sqrt{T^2 - 4U}^3},$$
$$\frac{\partial^2 \mu_{DA}}{\partial \mu_{AA} \partial \mu_{DD}} = 2\omega\xi \frac{\kappa T}{\sqrt{T^2 - 4U}^3}.$$

To update (E_m, K_d) we use the Nelder-Mead simplex algorithm (Nelder and Mead, 1965) as implemented in the routine *optim* in the statistical computing system R (R Development Core Team, 2012).

References

Chen, H., H. L. Puhl, and S. R. Ikeda (2007). Estimating protein-protein interaction affinity in living cells using quantitative Förster resonance energy transfer measurements. *Journal of Biomedical Optics 12*(5), 054011.

Chen, H., H. L. Puhl, S. V. Koushik, S. S. Vogel, and S. R. Ikeda (2006). Measurement of FRET efficiency and ratio of donor to acceptor concentration in living cells. *Biophysical journal 91*(5), 39–41.

Erickson, M. G., B. A. Alseikhan, B. Z. Peterson, and D. T. Yue (2001). Preassociation of calmodulin with voltage-gated Ca2+ channels revealed by FRET in single living cells. *Neuron 31*, 973–985.

Erickson, M. G., H. Liang, M. X. Mori, and D. T. Yue (2003). FRET twohybrid mapping reveals function and location of L-type Ca2+ channel CaM preassociation. *Neuron 39*, 97–107.

Markovsky, I. and S. V. Huffel (2007). Overview of total least squares methods. *Signal Processing 87*, 2283–2302.

Nelder, J. A. and R. Mead (1965). A simplex method for function minimization. *Computer Journal 7*, 308–313.

R Development Core Team (2012). *R: A Language and Environment for Statistical Computing*. Vienna, Austria: R Foundation for Statistical Computing. ISBN 3-900051-07-0.

Rasband, W. (1997–2012). *ImageJ*. Bethesda, Maryland, USA: U. S. National Institutes of Health. `http://imagej.nih.gov/ij/`.

Zal, T. and R. J. Gascoigne (2004). Photobleaching-corrected FRET efficiency imaging of live cells. *Biophysical journal 86*(6), 3923–3939.